



Oxide-bearing and FeO-rich clasts in aubrites

E. B. ROSENSHEIN^{1,2}, M. A. IVANOVA³, T. L. DICKINSON⁴, T. J. McCOY^{1*},
 D. S. LAURETTA⁵, Y. GUAN⁶, L. A. LESHIN⁶, and G. K. BENEDIX⁷

¹Department of Mineral Sciences, National Museum of Natural History, Smithsonian Institution, Washington, D.C. 20560–0119, USA

²Department of Geological and Environmental Sciences, Binghamton University, Binghamton, New York 13902, USA

³Laboratory of Meteoritics, Vernadsky Institute of Geochemistry, Kosygin St. 19, Moscow 119991, Russia

⁴The National Academies, Washington, D.C. 20001, USA

⁵Lunar and Planetary Laboratory, The University of Arizona, Tucson, Arizona 85721, USA

⁶Department of Geological Sciences, Arizona State University, Tempe, Arizona 85287–1404, USA

⁷Department of Earth and Planetary Sciences, Washington University, Saint Louis, Missouri 63130–4889, USA

*Corresponding author. E-mail: mccoyt@si.edu

(Received 02 June 2004; revision accepted 12 October 2005)

Abstract—We report the occurrence of an oxide-bearing clast and an FeO-rich clast from aubrites. The FeO-rich clast in Pesyanoe is dominated by olivine and pyroxene phenocrysts with mineral compositions slightly less FeO-rich than is typical for H chondrites. In Allan Hills (ALH) 84008, the oxide-bearing clast consists of a single forsterite grain rimmed by an array of sulfides, oxides, and phosphides. We consider a number of possible origins. We can exclude formation by melting of oxide-bearing chondrules and CAIs formed in enstatite chondrites. The Pesyanoe clast may have formed in a more oxidized region of the aubrite parent body or, more likely, is a foreign clast from a more oxidized parent body. The ALH 84008 clast likely formed by reaction between sulfides and silicates as a result of cooling, oxidation, or de-sulfidization. This clast appears to be the first oxide-bearing clast from an aubritic breccia that formed on the aubrite parent body. Identification of additional oxide-bearing clasts in aubrites could shed light on whether this was a widespread phenomenon and the origin of these enigmatic objects.

INTRODUCTION

Aubrites are breccias composed of igneous clasts, which are themselves dominated by FeO-free enstatite with minor to trace amounts of forsterite, feldspar, Si-bearing metal, and a diverse suite of unusual sulfides (e.g., oldhamite, alabandite, daubreelite) (see Mittlefehldt et al. 1998 and references therein). This mineral assemblage formed under extremely reducing conditions through a complex range of processes, including melting, melt migration, liquid immiscibility, cooling, crystallization, and exsolution. We initiated a petrographic study of aubritic clasts to look for FeNi and sulfides assemblages that might sample the aubrite partial melts. However, during the course of this study, we found an oxide-bearing and a FeO-rich clast (in Allan Hills [ALH] 84008 and Pesyanoe).

FeO-bearing clasts have been previously described in several aubrites. Chondritic clasts were found in the Cumberland Falls (Kallemeyn and Wasson 1985) and ALH 78113 aubrites (Lipschutz et al. 1988) and the latter also contains individual FeO-rich pyroxenes (Kimura et al. 1993).

The occurrence of these clasts in aubrites could indicate that a process that is yet unrecognized has occurred on the highly reduced aubrite parent body. This paper discusses the petrography and origin of these clasts.

SAMPLES AND TECHNIQUES

We surveyed every specimen of the ALH 84 aubrite pairing group (ALH 84007–84024) in the NASA Johnson Space Center Antarctic Meteorite Curatorial Facility as well as numerous specimens of the Pesyanoe aubrite from the collection of the Russian Committee on Meteorites to select specimens in which we could macroscopically identify metal and/or sulfides. Of particular initial interest were several samples of ALH 84008 that exhibited prominent pistachio-green weathering rinds indicative of terrestrial weathering of oldhamite (Wheelock et al. 1994). From the ALH 84 specimens, we prepared polished thin sections of ALH 84008 (numbers 73, 78, 79, 80, and 83), ALH 84014 (7) and ALH 84024 (14). We also studied a clast identified in a polished thin section of Bishopville (PTS USNM 222-1).

Selected clasts were studied by a variety of techniques. All clasts were examined in transmitted and reflected light. Energy dispersive analyses for phase identification, backscattered electron imaging, and X-ray elemental mapping were conducted on a JEOL JSM-840A scanning electron microscope and a JEOL JXA-8900R electron microprobe in the Department of Mineral Sciences at the National Museum of Natural History, Smithsonian Institution. Quantitative mineral analyses were conducted using the JEOL JXA-8900R electron microprobe. Analytical conditions were a 15 keV accelerating voltage, 20 nA beam current and a fully focused beam for silicates, sulfides, and phosphides. A 5- and 7-micron beam was used for the glass analyses in Pesyanoe to avoid volatility of Na. Well-characterized minerals and pure elements were used as standards. Typical detection limits are ~0.05 wt%. In many cases, we obtained only 1–3 analyses of small, rare phases within each clast. Some microprobe analysis totals for sulfides were low (96–98%). This has been a persistent problem in the analysis of aubritic sulfides (e.g., Larimer and Ganapathy 1987; Wheelock et al. 1994; Lodders 1996a, 1996b; Dickinson and McCoy 1997) and probably reflects the rapid weathering of the surface of these minerals and the lack of appropriate microprobe standards for these unusual compositions. In most cases, despite low totals, the calculated stoichiometries are close to the ideal. In the case of djerrfisherite, these problems were so severe that we were unable to obtain analyses for which the totals and stoichiometries were acceptable and we thus do not report the compositions of this mineral here.

Oxygen isotopes were analyzed using the CAMECA ims-6f ion microprobe at Arizona State University. A ~0.6 nA primary beam of Cs⁺ at +10 keV was focused into a spot ~20 μm in diameter in aperture illumination mode. Secondary ions were accelerated to -9 keV and collected by peak-jumping into either a Faraday cup (¹⁶O⁻) or electron multiplier (¹⁷O⁻ and ¹⁸O⁻) at a mass resolving power of ~6000, sufficiently resolving the ¹⁶OH⁻ interference on ¹⁷O⁻. A liquid nitrogen trap was used near the sample surface to further depress the hydride signal. Each analysis consisted of 30 cycles through the chosen masses and took ~20 min, including 5 min of pre-sputtering time. Instrumental mass fractionation was corrected using the Crestmore olivine standard (Hervig et al. 1992). Uncertainties on individual analyses, including analytical errors and statistical variation on repeated analyses of the standard, are ~1–2‰ (±2σ).

RESULTS

Oxide-Bearing Clast in Allan Hills 84008

In Allan Hills 84008 (PTS, 78), we have found an oxide-bearing clast. This clast measures ~800 × 400 μm. It is dominated by a single subhedral forsterite grain measuring 520 × 310 μm that is rimmed by an array of sulfides, oxides,

and phosphides (Fig. 1a). Enstatite is observed in igneous contact with forsterite. Three edges of the forsterite grain are rimmed by sulfides, dominantly troilite (1.28 wt% Ti) with lesser amounts of alabandite (Mn_{0.79}Fe_{0.16}Mg_{0.06}S), djerrfisherite, daubreelite, and schreibersite. The assemblage—enstatite, forsterite, sulfides, and schreibersite—is similar to many aubritic clasts, as are their average compositions (Tables 1, 2, and 3).

The presence of oxides of elements normally found as reduced sulfides in aubrites make this clast noteworthy. Both geikielite (ideally MgTiO₃) and perovskite (ideally CaTiO₃) are found within the clast (Fig. 1b). To the best of our knowledge, these phases have not been previously reported in aubrites. These phases occur within the troilite as grains of ~5–30 μm in diameter. The largest of these are composites of the two phases. These larger grains are dominantly geikielite ((Mg_{1.01}Fe_{0.01})_{Σ = 1.02}Ti_{0.99}O₃) with 1–5 μm inclusions of perovskite ((Ca_{0.94}Mg_{0.05}Fe_{0.02})_{Σ = 1.01}Ti_{0.99}O₃) (Fig. 1c). Given their small size, some of the Mg in the perovskite probably results from beam overlap with the host geikielite.

Equally unusual is an intergrowth which appears to replace approximately one-third of the forsterite grain (Fig. 1d). This intergrowth is extremely fine-grained, with most phases in the range of 2 μm or less. Thus, quantitative analysis using the electron microprobe was not possible. We have determined the mineralogy using a variety of techniques, including optical microscopy, BSE imaging, energy dispersive qualitative analyses on the SEM, and elemental mapping using the microprobe. These methods suggest that the bulk of the intergrowth is troilite and diopside. Perovskite is also found within the intergrowth, particularly at the boundary between the intergrowth and the host forsterite. TEM studies might shed further light on the mineral chemistry in the intergrowth, but were beyond the scope of this study.

FeO-Rich Clast in Pesyanoe

In the Pesyanoe aubrite, we discovered a compositionally unusual FeO-rich clast. It is texturally similar to other pyroxenitic clasts found in the Pesyanoe breccia. The clast, measuring 420 × 230 μm (Fig. 2), occurs on the edge of the polished section and has an irregular shape. Mineralogically, it is dominated by olivine and pyroxene phenocrysts (20–50 μm in size) in an interstitial SiO₂-rich glass containing minute troilite inclusions (up to 3 μm). The modal composition of the clast is 40.4% olivine, 40.3% pyroxene, 18.2% glass, and 1.0% troilite. In general, the boundary between the clast and Pesyanoe host is easily distinguished. However, single grains of diopside and plagioclase occur along one edge of the clast adjacent to the polished section edge, and their relationship to the clast is ambiguous.

In contrast to the essentially FeO-free silicates typical of aubrites, this clast contains FeO-rich silicates-olivine (Fa_{14.4}), orthopyroxene (Fs_{13.2}Wo_{3.0}), and pigeonite (Fs_{12.3}Wo_{7.9})

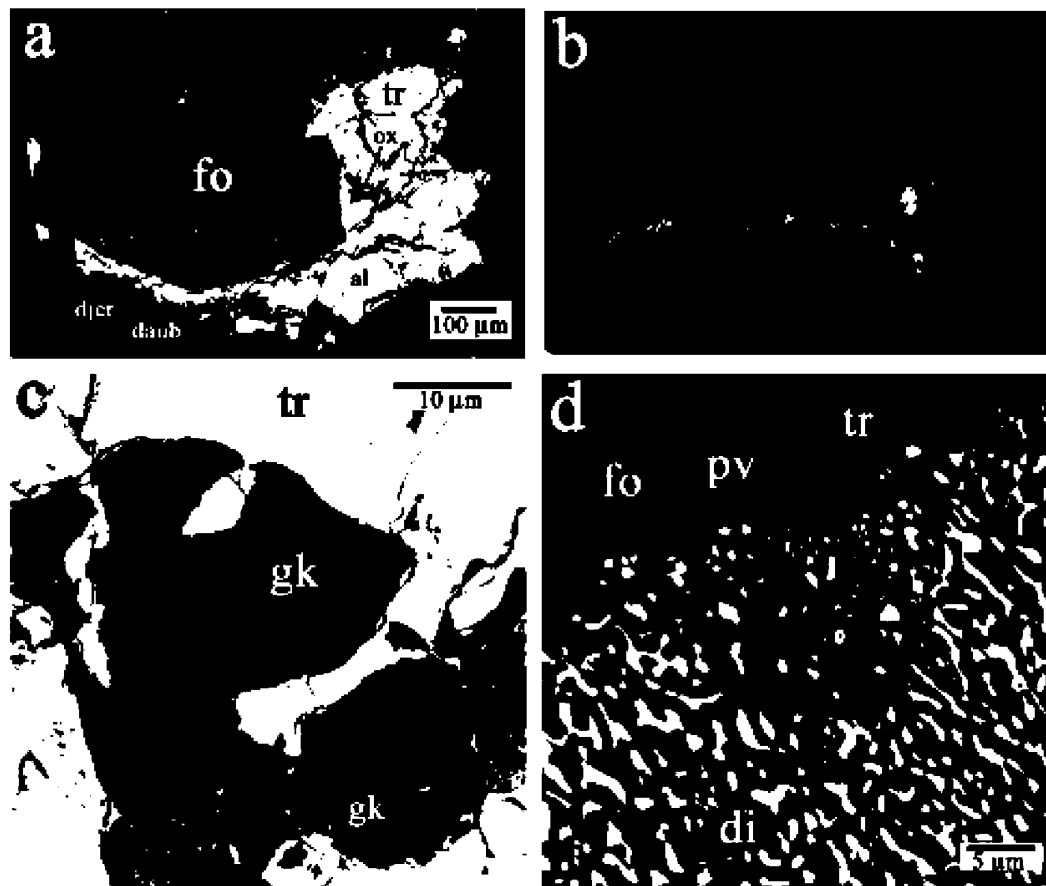


Fig. 1. The oxide-bearing clast in ALH 84008. a) A reflected light photomicrograph of the entire clast. The clast is dominated by a single, subhedral forsterite (fo) grain, rimmed by Ti-bearing troilite (tr), alabandite (al), daubreelite (daub), and djerfisherite (djer). Within the Ti-bearing troilite are compound grains of the oxides (ox) geikielite and perovskite. The forsterite grain is partially replaced with an intergrowth (in) of diopside, troilite, and perovskite. b) A Ti X-ray map of the clast. Bright spots indicate Ti-rich oxide phases (geikielite and perovskite) as distinct grain in the troilite and within the troilite-diopside-perovskite intergrowth. c) A BSE image of geikielite (gk) and perovskite (pv) grains within troilite (tr). d) A BSE image of the intergrowth of diopside (di), troilite (tr), and perovskite (pv) that is bordering the large forsterite (fo) grain. This unusual Ti-rich oxide assemblage may have formed by oxidation of elements that are normally found in reduced sulfides in aubrites.

(Table 1). These compositions are only slightly less FeO-rich than typical for H chondrite silicates and similar to those of in the silicate-bearing Netschaevite IIE iron (Bild and Wasson 1977) and the low-FeO chondrite Burnwell (Russell et al. 1998) (Fig. 3).

The interstitial mesostasis in the clast appears to be a glass enriched in SiO_2 compared to feldspar, with a range of SiO_2 (71–88 wt%) and Al_2O_3 (7–19 wt%). Our analyses suggest a bimodal composition, with one richer in SiO_2 and Na_2O and poorer in TiO_2 , Al_2O_3 , FeO, CaO, and K_2O . These compositions may suggest an origin as immiscible liquids. The Na_2O and K_2O differences may be due to volatilization during analysis. However, it is unlikely that the other elemental differences are caused by volatilization.

Troilite from the Pesyanoe aubritic host contains significant amounts of Ti (0.46 wt%) (Watters and Prinz 1979). The troilite grains in this clast appear to lack Ti based on qualitative EDS spectra. These grains are very small ($\leq 3 \mu\text{m}$),

and thus we were unable to obtain reliable quantitative analyses. The clast did not contain any metal grains.

Oxygen Isotopic Compositions

Oxygen isotopic analyses of the ALH 84008 clast are illustrated in Fig. 4 along with analyses of bulk aubrites from Clayton and Mayeda (1996). We analyzed olivine both inside and outside of the clast. The replicate isotopic measurements for the clast are $\delta^{17}\text{O} = 0.99\text{‰}$ and $\delta^{18}\text{O} = 3.28\text{‰}$, and $\delta^{17}\text{O} = 2.57\text{‰}$ and $\delta^{18}\text{O} = 5.31\text{‰}$. The values for the host are $\delta^{17}\text{O} = 1.73\text{‰}$ and $\delta^{18}\text{O} = 1.73\text{‰}$, and $\delta^{17}\text{O} = 2.13\text{‰}$ and $\delta^{18}\text{O} = 1.85\text{‰}$. Our analyses of the clast and host in ALH 84008 are within the range observed for bulk aubrites ($\delta^{18}\text{O} \sim 5.0\text{--}5.5\text{‰}$ and $\delta^{17}\text{O} \sim 2.6\text{--}2.9\text{‰}$) and are identical within analytical uncertainty ($\sim 1\text{--}2\text{‰}$). One of the clast values fall almost exactly on the values measured for aubrites (Clayton and Mayeda 1996).

Table 1. The average compositions (wt%) of silicates and oxides in the oxide-bearing clast in ALH 84008 and silicates and glass in Pesyanoc. Values in parentheses are 1σ of compositional variability of N analyses in the last decimal place (unless otherwise noted).

	Oxide-bearing clast ALH 84008				FeO-rich clast Pesyanoc				
	Forsterite	Enstatite	Geikielite	Perovskite	Olivine	Orthopyroxene	Pigeonite	K-poor glass	K-rich glass
SiO ₂	41.4(2)	57.9(1)	b.d.	b.d.	40.2 (4)	56.0 (2)	55.2 (6)	84.8 (4.0)	72.5 (8)
TiO ₂	b.d.	b.d.	64.5(4)	57.2	n.d.	n.d.	n.d.	0.06 (3)	0.46 (1)
Al ₂ O ₃	b.d.	0.08(1)	b.d.	b.d.	n.d.	n.d.	n.d.	8.3 (2.3)	19.2 (2)
Cr ₂ O ₃	n.d.	n.d.	n.d.	n.d.	0.19 (6)	0.53 (12)	0.60 (3)	n.d.	n.d.
FeO	0.16(15)	0.11(2)	0.77(14)	1.38	13.5 (5)	8.8 (3)	7.8 (2)	0.20 (2)	0.54 (5)
MnO	b.d.	b.d.	b.d.	b.d.	0.41 (6)	0.43 (4)	0.37 (2)	n.d.	n.d.
MgO	58.3(3)	40.3(1)	33.5(1)	1.38	44.8 (4)	31.3 (6)	28.7 (2.1)	b.d.	0.21 (13)
CaO	b.d.	0.53(5)	b.d.	38.0	0.21 (3)	1.55 (58)	4.0 (1.0)	b.d.	1.11 (7)
Na ₂ O	b.d.	b.d.	b.d.	0.10	n.d.	n.d.	n.d.	4.4 (1.8)	0.57 (54)
K ₂ O	n.d.	n.d.	n.d.	n.d.	n.d.	n.d.	n.d.	0.25 (5)	1.53 (12)
Total	99.86	98.92	98.77	98.06	99.29	98.59	97.84	95.69	96.16
N	6	2	2	1	9	5	4	2	4

b.d. = below detection limit; n.d. = not determined.

Table 2. Average compositions (wt%) of sulfides in the oxide-bearing clast in ALH 84008. Values in parentheses are 1σ of compositional variability of N analyses in the last decimal place (unless otherwise noted).

	Oxide-bearing clast ALH 84008		
	Troilite	Alabandite	Daubreelite
Fe	62.5(3)	10.1(1.5)	18.6(1)
Mn	b.d.	49.3(1.2)	1.03(14)
Mg	b.d.	1.53(7)	b.d.
Ca	b.d.	0.12(1)	b.d.
Ti	1.28(18)	b.d.	0.08(1)
Cr	0.36(5)	b.d.	34.6(8)
Cu	b.d.	b.d.	0.09(5)
S	35.6(2)	36.2(1)	41.7(1.9)
Total	99.74	97.25	96.1
N	8	4	2

b.d. = below detection limit.

Table 3. Average compositions (wt%) of schreibersite in the oxide-bearing clast in ALH 84008. Values in parentheses are 1σ of compositional variability of N analyses in the last decimal place (unless otherwise noted).

	Oxide-bearing clast ALH 84008
	Schreibersite
Fe	39.0(1.0)
Ni	44.7(2.0)
Si	0.66(55)
Co	b.d.
P	15.0(5)
Total	99.36
N	2

b.d. = below detection limit.

DISCUSSION

Most aubrites contain calcium in oldhamite and diopside, magnesium in enstatite, forsterite, diopside, and alabandite, and titanium in diopside, titanite, troilite, and osbornite (TiN). The occurrence of the oxide-bearing clasts in ALH 84008 and FeO-bearing clasts in Pesyanoc is unexpected. We discuss a number of possible models for their formation. There may be no unique model to explain their origin and there is no reason to believe that both clasts formed in the same manner. We believe that a few possible origins can be excluded based on the evidence presented in this paper.

Derived from Oxide-Bearing Material from Enstatite Chondrites

Geikielite and perovskite, although not previously observed in aubrites, are known to occur in calcium-aluminum-rich inclusions (CAIs) in enstatite chondrites (Fagan et al. 2000; Guan et al. 2000; Lusby et al. 1987). Is it possible that these phases in ALH 84008 are relict grains from an enstatite chondrite CAI that survived igneous processing on the aubrite parent body? In support of such an idea is the fact that perovskite is highly refractory, with a melting temperature as a pure substance approaching 1975 °C (Weast 1970). However, perovskite in the intergrowth is intimately associated with troilite and diopside, quite unlike what one would expect of a relict phase. We therefore find such an origin unlikely.

An alternative to the relict hypothesis is that an oxide-bearing CAI or FeO-rich chondrule from the enstatite chondrite-like aubrite protolith melted and during igneous processing remained an essentially immiscible liquid, ultimately crystallizing to produce these clasts. There are a

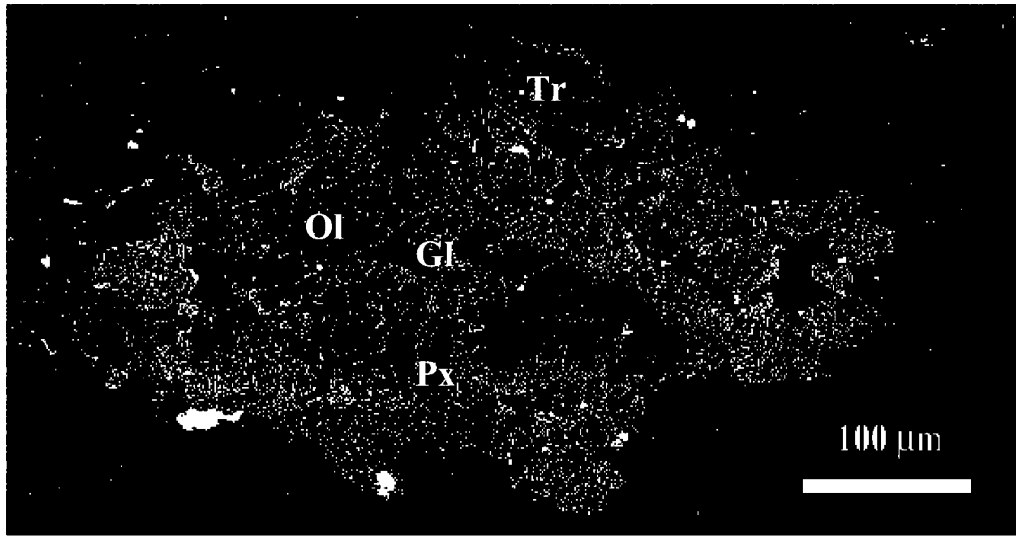


Fig. 2. A backscattered electron image of FeO-rich clast from Pesyanoe aubrite. The clast contains olivine (Ol), pyroxene (Px), glass (Gl), and troilite (Tr) and has a very distinguishable boundary with material of the Pesyanoe host.

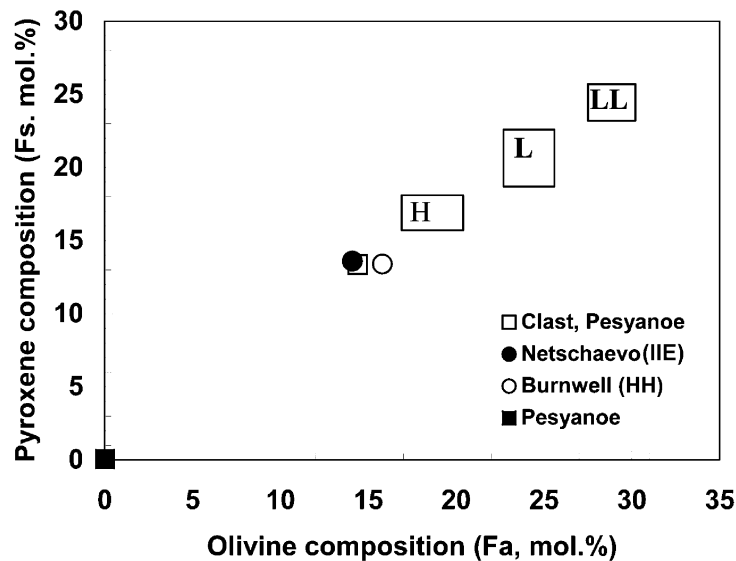


Fig. 3. The chemical composition of olivine and low-Ca pyroxene from FeO-rich clast. These compositions are only slightly less FeO-rich than is typical for H-chondrite silicates and is similar to those of in the silicate-bearing Netschaevo IIE iron (Bild and Wasson 1977) and the low-FeO chondrite Burnwell (Russell et al. 1998).

variety of reasons to question such a model, including the likely homogenization of compositions during pre-melting metamorphism and the instability of such a melt (both chemically and thermally) within a large, dynamic magma system. While we cannot completely exclude such an origin, we find it unlikely.

Origin in a More Oxidized Part of the Aubrite Parent Body

These clasts could have formed in a region of the aubrite parent body that was inherently more oxidizing and

which we are only now recognizing from these apparently rare clasts. This idea raises a number of important questions: why was some part of the parent body more oxidizing? What is the precursor for this oxidized area? How extensive was such a region? The data for the ALH 84008 clast, which contains several highly reduced phases typical of aubrites, does not support this idea. These phases must have formed in a reducing environment. Such an idea could work for the Pesyanoe clast, which exhibits none of the reduced features typical of aubrites. However, we believe a more likely explanation exists for the origin of the Pesyanoe clast.

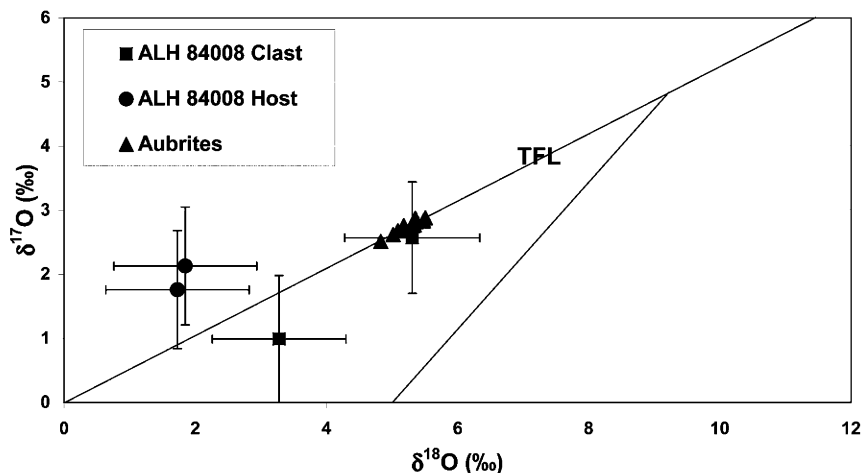


Fig. 4. Oxygen isotopic analyses of oxidized clasts in ALH 84008 and aubrites (Clayton and Mayeda 1996).

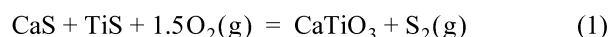
Foreign Source

Aubrites are breccias, many of which contain regolith components (Keil 1989). As we noted earlier, at least some of these components are clearly foreign and originated on the parent bodies of oxidized chondritic meteorites. Perhaps these clasts are unrelated to the aubrite parent body, but rather were admixed during collision of a more oxidized impactor. For the oxide-bearing clast in ALH 84008, this seems unlikely because most of the minerals found in the clast—essentially FeO-free forsterite and enstatite, titanite, troilite, alabandite, and djerfisherite—are typical of an enstatite meteorite assemblage and are rare or unknown in more oxidized meteorites in which perovskite and geikielite are abundant (Brearley and Jones 1998). Such an origin deserves more serious consideration in the case of the Pesyanoe clast, given the lack of reduced minerals and the compositional similarity to oxidized ordinary chondrites. Support for this hypothesis comes from the recent discovery of additional FeO-rich and carbonaceous chondrite clasts from Pesyanoe (Lorenz et al. 2005). It is possible that the slightly lower FeO concentrations in olivine and pyroxene within this clast reflect partial equilibration between the clast and its highly reduced host, akin to that suggested for Galim (a) and (b) by Rubin (1997).

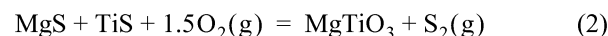
Formation of ALH 84008 by Reaction

The ALH 84008 clast is unusual for aubrites in that it contains oxide-bearing material. Most notably, this clast contains oxides of Mg, Ca, and Ti, elements that are commonly chalcophile in aubrites. This clast probably represents a distinct microenvironment on the aubrite parent body. In order to understand the conditions recorded by these minerals, we considered several possible chemical reactions, which may have been responsible for their formation. ALH 84008 contains perovskite and geikielite as inclusions in

troilite. The formation of these phases can be described individually using the reactions:

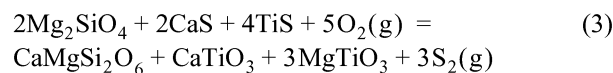


and



The existence of CaS (oldhamite) and MgS (in a solution in alabandite) as a precursor phase to this clast is hypothesized, although no remnants of these phases exist in association with perovskite or geikielite. Oldhamite does occur in some abundance in ALH 84008, as does Mg-bearing alabandite. Reactions 1 and 2 illustrate the importance of the fugacities of both oxygen and sulfur in determining the stability of the oxide phases found in these rare aubrites clasts. In addition, equilibrium constants for reactions such as those presented above are temperature dependent. Thus, significant changes in temperature, f_{O_2} , or f_{S_2} could result in production of the oxides. Since these minerals occur in intimate association with silicates, we prefer to model the system using a net chemical reaction involving sulfides, silicates, and oxides.

A reaction origin for the oxide-bearing clast in ALH 84008 is suggested by the texture of the intergrowth, where a subhedral forsterite grain appears to have reacted with enveloping sulfides to produce a troilite-diopside-perovskite intergrowth (Fig. 1a). A net chemical reaction describing this assemblage is:



Again, we hypothesize the existence of CaS (oldhamite) in the precursor assemblage, although no oldhamite exists in the current ALH 84008 clast. The equilibrium constant for Reaction 3 can be expressed as:

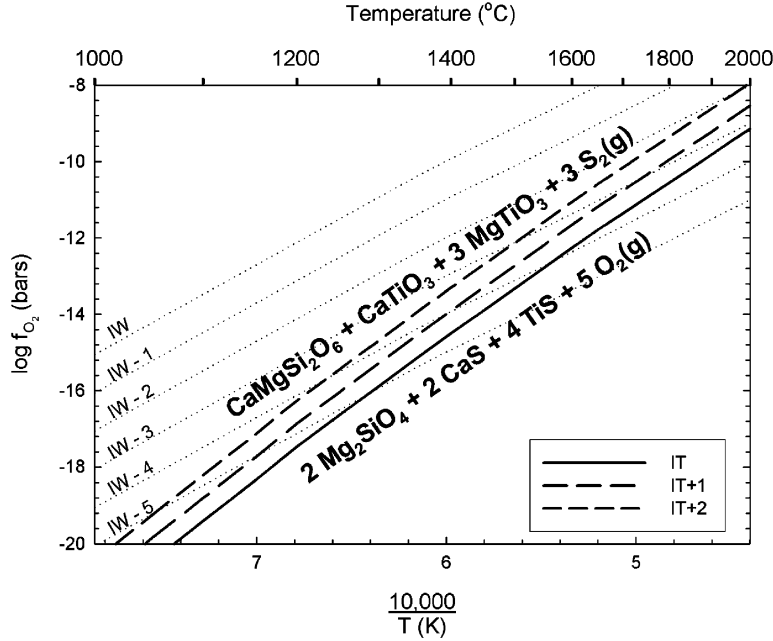


Fig. 5. A graph illustrating the dependence of Reaction 3 on f_{O_2} , f_{S_2} , and temperature. Oxygen fugacities relative to the iron-wüstite (IW) buffer are shown as dotted lines. The effect of f_{S_2} is illustrated by plotting the reaction curves (solid and dashed lines) for different values, relative to the iron-troilite (IT) buffer.

$$\log K_3 = \log a_{\text{CaMgSi}_2\text{O}_6}^{\text{Cpx}} + \log a_{\text{CaTiO}_3}^{\text{Pv}} + 3 \log a_{\text{MgTiO}_3}^{\text{Gk}} + 3 \log f_{S_2} - 2 \log a_{\text{Mg}_2\text{SiO}_4}^{\text{Oliv}} - 2 \log a_{\text{CaS}}^{\text{Old}} - 4 \log a_{\text{TiS}}^{\text{Troil}} - 5 \log f_{O_2} \quad (1)$$

$$\log f_{O_2} = \frac{3}{5} \cdot \log f_{S_2} - \frac{27,902}{T} + 4.54 \quad (5)$$

where a_c^i is the activity of component c in phase i . Using tabulated thermodynamic data from Barin (1995) for $\text{CaMgSi}_2\text{O}_6$ and MgTiO_3 , from Knacke et al. (1991) for Mg_2SiO_4 , Glushko (1994), from SGTE (1999) for CaS , MgS , TiS , and from Woodfield et al. (1999) for CaTiO_3 , this equation can be expressed in the form:

$$\log K_3 = \frac{A}{T} + B \quad (2)$$

where T is the temperature in Kelvin from 1273–2273. We calculate values for A and B of 139,508 and -16.18 , respectively, producing the equation:

$$\log K_3 = \frac{139,508}{T} - 16.18 \quad (3)$$

By equating Equations 1 and 3 and assuming that the activity of all solid phases is unity, except for TiS , where we use a value of 0.024 for a_{TiS} , equivalent to its mole fraction in troilite determined by electron microprobe analyses, we produce an equation of the form:

$$\frac{139,508}{T} - 16.18 = 3 \log f_{S_2} - 4 \log(0.024) - 5 \log f_{O_2} \quad (4)$$

Solving for $\log f_{O_2}$ and simplifying the equation, we find:

Equation 5 shows that the stability of the various oxide and sulfide phases depends on both the oxygen fugacity (f_{O_2}) and sulfur fugacity (f_{S_2}). Higher f_{O_2} values will drive the reactions to the right while increasing f_{S_2} will drive them to the left. We plot the results of these calculations in Fig. 5 as a function of temperature and f_{S_2} . By analogy with the iron-wüstite system, we use the iron-troilite sulfur fugacity buffer to describe f_{S_2} values. The relevant reaction is:



We use the petrography of the samples to put some constraints on the f_{S_2} values relevant to aubrites. The temperatures that we are interested in are above the Fe-FeS eutectic (1261 K). Thus, the sulfur fugacity should be that in equilibrium with the Fe-FeS melt. However, f_{S_2} varies significantly with the S content of the melt. According to the phase diagrams presented in Naldrett (1989), at 1723 K, an Fe-S melt with a S content of 28 wt% results in an f_{S_2} of 10^{-4} bars (IT $- 0.3$). Increasing the S content to 36 wt% (appropriate to the dominance of troilite and alabandite within the enveloping sulfides) yields an f_{S_2} of 10^{-1} bars (IT $+ 2.7$). Thus, it is apparent that the f_{S_2} is highly dependent on the Fe-S melt composition. Given this variation, we consider f_{S_2} values ranging from IT to IT $+ 2$ in the calculations shown in Fig. 5. These calculated stability curves are similar to those predicted for Reactions 1 and 2.

These calculations suggest several possible origins for the ALH 84008 clast. The most obvious possibility is that the complex precursor assemblage required—forsterite, oldhamite, and titanite—occur together so infrequently that this reaction has never been previously observed. We find such an explanation unlikely. Although all three are trace to minor phases in aubrites, troilite and forsterite occur at the 1–10 vol% level in aubrites and oldhamite at the fractions of a percent level. Thus, it seems that other occurrences of this interaction should have been previously noted.

The second possibility is that such a reaction occurred as a result of cooling of this assemblage at an oxygen fugacity appropriate to aubrites (~IW-5) (Casanova et al. 1993). At this fO_2 and an fS_2 of IT + 2, reaction between forsterite, oldhamite, and titanite would produce perovskite, geikelite, and diopside at ~1050 °C. We cannot rule out such an origin, although it should have occurred during cooling of any forsterite-oldhamite-troilite assemblage at ambient fO_2 and fS_2 conditions. We would also note that the liquidus temperature of the complex sulfide assemblage seen in the ALH 84008 clast is highly uncertain. Reaction between solid sulfide and solid forsterite would probably be inhibited by kinetic barriers.

Increasing the fO_2 would also result in oxidation of the major sulfide phases and is intuitively the most obvious mechanism for producing oxide-bearing clasts in aubrites. As an example, changing the fO_2 from IW-5 to IW-4 at a constant fS_2 of IT + 2 and temperature of 1200 °C would produce the reaction hypothesized for ALH 84008. However, it is not clear what would drive this reaction. It is also possible that the system experienced a “de-sulfurizing” event, causing the fS_2 to drop. For example, at 1200 °C, a decrease from IT + 2 to IT at a constant fO_2 of IW-5 would result in oxidation of the assemblage. Such a scenario is possible if a fresh reservoir of metal became available to the system. At a fS_2 of IT + 2 this metal would sulfidize removing S_2 out of the gas phase. Distal sulfide assemblages would then degas S thus maintaining an equilibrium fS_2 . The bulk fS_2 of the system would decrease down to it. The subsequent oxidation reactions would continue until the fresh metal and the original sulfide assemblages were altered into metal-sulfide assemblages. This scenario is similar to the one described in Lauretta et al. (1997) based on experimental studies of sulfur mobilization under conditions relevant to ordinary chondrites.

CONCLUSIONS

We have identified an oxide-bearing and an FeO-rich clast from aubrites. We suggest that the Pesyanoe clast joins a growing list of foreign clasts derived from oxidized, chondritic asteroids that were admixed into the regolith of the aubrite parent body. In contrast, the ALH 84008 clast appears to be the first oxide-bearing clast formed on the aubrite parent

body. We suggest that it formed by reaction between sulfides and silicates as a result of cooling, oxidation or desulfidization. At this point, we cannot constrain a unique origin. We suggest that identification of additional oxide-bearing clasts in aubrites could shed light on whether oxidation was a widespread phenomenon on the aubrite parent body.

Acknowledgments—We thank Kathleen McBride and Cecilia Satterwhite (NASA/JSC) for invaluable assistance during sample selection and Kevin Righter and Robert Fogel for their thoughtful reviews. Technical assistance by Amelia Logan, Tim Gooding, and Eugene Jarosewich is appreciated. Funding was provided by NASA Cosmochemistry Grants NAG 5-4490 (TJM) and 5-4345, 5-8508, and 5-12993 (TLD), National Science Foundation Research Experiences for Undergraduates in the Geosciences Award EAR-9732416 and the Research Training Program of the National Museum of Natural History (EBR).

Editorial Handling—Dr. Ian Franchi

REFERENCES

- Barin I. 1995. *Thermochemical data of pure substances*. Weinheim, Germany: VCH Publishers. 1885 p.
- Bild R. W. and Wasson J. T. 1977. Netschaev—A new class of chondritic meteorite. *Science* 197:58–62.
- Brearley A. J. and Jones R. H. 1998. Chondritic meteorites. In *Planetary materials*, edited by Papike J. J. Washington, D.C.: Mineralogical Society of America. pp. 3-1–3-398.
- Casanova I., Keil K., and Newsom H. E. 1993. Composition of metal in aubrites: Constraints on core formation. *Geochimica et Cosmochimica Acta* 57:675–682.
- Clayton R. N. and Mayeda T. K. 1996. Oxygen isotope studies of achondrites. *Geochimica et Cosmochimica Acta* 60:1999–2017.
- Dickinson T. L. and McCoy T. J. 1997. Experimental rare-earth-element partitioning in oldhamite: Implications for the igneous origin of aubritic oldhamite. *Meteoritics & Planetary Science* 32: 395–412.
- Fagan T. J., Krot A. N., and Keil K. 2000. Calcium-aluminum-rich inclusions in enstatite chondrites (I): Mineralogy and textures. *Meteoritics & Planetary Science* 35:771–781.
- Glushko V. P. 1994. Thermocenter of the Russian Academy of Sciences, IVTAN Association, Izhorskaya 13/19, 127412 Moscow, Russia.
- Guan Y., Huss G. R., MacPherson G. J., and Wasserburg G. J. 2000. Calcium-aluminum-rich inclusions from enstatite chondrites: Indigenous or foreign? *Science* 289:1330–1333.
- Hervig R. L., Williams P., Thomas R. M., Schauer S. N., and Steele I. M. 1992. Microanalysis of oxygen isotopes in insulators by secondary ion mass spectrometry. *International Journal of Mass Spectrometry and Ion Processes* 120:45–63.
- Kallemeyn G. W. and Wasson J. T. 1985. The compositional classification of chondrites. IV. Ungrouped chondritic meteorites and clasts. *Geochimica et Cosmochimica Acta* 49:261–270.
- Keil K. 1989. Enstatite meteorites and their parent bodies. *Meteoritics* 24:195–208.
- Kimura M., Lin Ya.-T., Ikeda Yu, El Goresy A., Yanai K., and Kojima H. 1993. Mineralogy of Antarctic aubrites, Yamato

- 793592 and Allan Hills 78113: Comparison with non-Antarctic aubrites and E chondrites. *Proceedings of the NIPR Symposium on Antarctic Meteorites* 6:186–203.
- Knacke O., Kubaschewski O., and Hesselman K. 1991. *Thermochemical properties of inorganic substances*, 2nd ed. Berlin: Springer-Verlag. 1113 p.
- Larimer J. W. and Ganapathy R. 1987. The trace element chemistry of CaS in enstatite chondrites and some implications regarding its origin. *Earth and Planetary Science Letters* 84:123–134.
- Lauretta D. S., Lodders K., Fegley B., Jr., and Kremser D. T. 1997. The origin of sulfide-rimmed metal grains in ordinary chondrites. *Earth and Planetary Science Letters* 151:289–301.
- Lipschutz M. E., Verkontern R. M., Sears D. W. G., Hasan F. A., Prinz M., Weisberg M. K., Nehru C. E., Delaney J. S., Grossman L., and Boily 1988. Cumberland Falls chondritic inclusion: III. Consortium study relationship to inclusions in Allan Hills 78113 aubrite. *Geochimica et Cosmochimica Acta* 52: 1835–1848.
- Lodders K. 1996a. Oldhamite in enstatite achondrites (aubrites). *Proceedings of the NIPR Symposium on Antarctic Meteorites* 9: 127–142.
- Lodders K. 1996b. An experimental and theoretical study of rare-earth-element partitioning between sulfides (FeS, CaS) and silicate and applications to enstatite achondrites. *Meteoritics & Planetary Science* 31:749–766.
- Lorenz C. A., Ivanova M. A., Kurat G., and Brandstaetter F. 2005. FeO-rich xenoliths in the Staroye Pesyanoe aubrite (abstract #1612). 36th Lunar and Planetary Science Conference. CD-ROM.
- Lusby D., Scott E. R. D., and Keil K. 1987. Ubiquitous high-FeO silicates in enstatite chondrites. *Proceedings, 17th Lunar and Planetary Science Conference*. pp. E679–E695.
- Mittlefehldt D. W., McCoy T. J., Goodrich C. A., and Kracher A. 1998. Non-chondritic meteorites from asteroidal bodies. In *Planetary materials*, edited by Papike J. J. Washington, D.C.: Mineralogical Society of America. pp. 4–1–4–195.
- Naldrett A. J. 1989. *Magmatic sulfide deposits*. New York: Oxford University Press. 186 p.
- Rubin A. E. 1997. The Galim LL/EH polymict breccia: Evidence for impact-induced exchange between reduced and oxidized meteoritic material. *Meteoritics & Planetary Science* 32:489–492.
- Russell S. S., McCoy T. J., Jarosewich E., and Ash R. D. 1998. The Burnwell, Kentucky, low-FeO chondrite fall: Description, classification and origin. *Meteoritics & Planetary Science* 33: 853–856.
- Scientific Group Thermodata Europe (SGTE). 1999. *Thermodynamic properties of inorganic materials*. Berlin: Springer-Verlag. 415 p.
- Watters T. R. and Prinz M. 1979. Aubrites: Their origin and relationship to enstatite chondrites. *Proceedings, 10th Lunar and Planetary Science Conference*. pp. 1073–1093.
- Weast R. C. 1970. *Handbook of chemistry and physics*. Cleveland, Ohio: The Chemical Rubber Company. p. B-79.
- Wheelock M. M., Keil K., Floss C., Taylor G. J., and Crozaz G. 1994. REE geochemistry of oldhamite-dominated clasts from the Norton County aubrite: Igneous origin of oldhamite. *Geochimica et Cosmochimica Acta* 58:449–458.
- Woodfield B. F., Shapiro J. L., Stevens R., Boerio-Goates J., Putnam R. L., Helean K. B., and Navrotsky A. 1999. Molar heat capacity and thermodynamic functions for CaTiO₃. *Journal of Chemical Thermodynamics* 31:1573–1583.